This is a “preproof” accepted article for *Mineralogical Magazine*.
This version may be subject to change during the production process.
10.1180/mgm.2024.97

Paragenesis, composition and origin of Ba- and Ca-rich stronalsite, a rare strontium tectosilicate, in the rocks of the teschenite association, Silesian Unit, Western Carpathians, Czech Republic

Kamil KROPÁČ[1], Zdeněk DOLNÍČEK[2*], Jana ULMANOVÁ[2]

[1] Department of Geology, Faculty of Science, Palacký University, 17. listopadu 12, 771 46 Olomouc, Czech Republic

[2] Department of Mineralogy and Petrology, National Museum, Cirkusová 1740, 193 00 Prague 9, Czech Republic

[*]Corresponding author. E-mail: zdenek.dolnicek@nm.cz

Abstract

The Ba- and Ca-rich stronalsite [ideally $SrNa_2Al_4Si_4O_{16}$] rarely occurs in pseudomorphs probably after nepheline in hydrothermally altered Sr-enriched leucocratic dykes or streaks hosted by mesocratic amphibole-pyroxene teschenite in the Silesian Unit (Flysch Belt of the Western Carpathians, Czech Republic). In addition to stronalsite, the pseudomorphs consist of slawsonite, celsian, biotite, muscovite, alkali feldspar, natrolite, and thomsonite-Ca. The surrounding groundmass is rich in alkali feldspars and zeolites and sporadically also contains amphibole phenocrysts, chloritized biotite, fluorapatite and other accessory and/or secondary minerals. Both compositional types of stronalsite show identical Raman spectra. The Ba-rich stronalsite contains 0.55–0.83 apfu Sr, 0.12–0.37 apfu Ba, and <0.08 apfu Ca. In contrast, Ca-rich stronalsite contains 0.65–0.82 apfu Sr, 0.10–0.23 apfu Ca, and <0.06 apfu Ba. The substitution mechanisms by which Ca enters the structure of stronalsite could not be satisfactorily clarified from the available data; the best stoichiometric fit suggests for substitution of Sr, which should not be allowed due to different crystal structure of Ca-analog of stronalsite, lisetite [ideally $CaNa_2Al_4Si_4O_{16}$]. The Na contents range 1.82–2.42 apfu and the K contents are always low (<0.09 apfu). The *T* site contains 3.91–4.26 apfu Si, 3.76–4.00 apfu Al and 0.00–0.11 apfu Fe^{3+}. The main source of Sr was probably primary magmatic plagioclase, which underwent hydrothermal alteration by post-magmatic high-temperature brines mixed with fluids of external origin. Based on previous research and paragenetic relationships, we estimate that stronalsite crystallized at T ~250–320 °C and P <100 MPa.

Keywords: stronalsite, slawsonite, strontium, hydrothermal alteration, teschenite, Silesian Unit, Outer Western Carpathians

Introduction

Stronalsite [$SrNa_2Al_4Si_4O_{16}$] is a rare orthorhombic tectosilicate from the Feldspar Group. Its ideal formula can be derived from the simple addition of one molecule of slawsonite [$SrAl_2Si_2O_8$] and two molecules of K-free nepheline [$NaAlSiO_4$] (Hori *et al.*, 1987). Two other tectosilicates show similar stoichiometry $ANa_2Al_4Si_4O_{16}$: banalsite [$BaNa_2Al_4Si_4O_{16}$] (Campbell Smith *et al.*, 1944a,b) and lisetite [$CaNa_2Al_4Si_4O_{16}$] (Rossi *et al.*, 1986). Stronalsite forms a solid-solution series with banalsite (Koneva, 1996; Liferovich *et al.*, 2006a,b). In contrast, the miscibility with lisetite should be restricted due to differences in their crystal structures (Liferovich *et al.*, 2006a,b). Stronalsite and banalsite crystallize in space group *Iba*2 (Matsubara, 1985; Hori *et al.*, 1987; Liferovich *et al.*, 2006a) and lisetite in space group $Pbc2_1$ (Rossi *et al.*, 1986). The basic framework of both *Iba2*- and $Pbc2_1$-structured tectosilicates is topologically similar (Si and Al cations are fully ordered in tetrahedral positions and build up four-fold and eight-fold rings consisting of vertex-sharing tetrahedrons arranged in –UDUD– sequence; Liferovich *et al.*, 2006a), however, the location of large intra-framework cations differ in both structures. In stronalsite and banalsite, ordered ^{X}Ba or ^{X}Sr and ^{VI}Na cations form alternating layers parallel to (001) and shifted by ¼ *c* (Liferovich *et al.*, 2006a; Fig. 1a), whereas ^{VII}Ca and ^{VI}Na cations in lisetite are distributed throughout common Ca + 2Na layers (Rossi *et al.*, 1986; Fig. 1b).

The occurrence of tectosilicates with stoichiometry $ANa_2Al_4Si_4O_{16}$ is related to high-grade metamorphic and metasomatic rocks (Campbell Smith *et al.*, 1944a,b; Smith *et al.*, 1986; Hori *et al.*, 1987), altered Si-poor alkaline igneous rocks (predominantly nepheline syenites),

ultramafic xenoliths in alkaline rocks, and alkaline ultramafic rocks, often associated with carbonatites (Khomyakov *et al.*, 1990; Koneva, 1996; Dunworth and Bell, 2003; Liferovich *et al.*, 2006b; Dahlgren and Larsen, 2012). Banalsite was identified for the first time by Campbell Smith *et al.* (1944a,b) from the Benallt manganese mine in the Llŷn Peninsula (Wales), whereas lisetite was described by Smith *et al.* (1986) from the Liset eclogite pod in Selje (Norway). The first occurrence of stronalsite was described by Hori *et al.* (1983, 1987) and Matsubara (1985) in a pectolite–slawsonite veinlet intersecting mafic metatuff xenolith in serpentinite at Rendai (Kochi Prefecture, Japan). Hori *et al.* (1987) also validated the second occurrence of stronalsite in a jadeite–serpentine rock at Mt. Ohsa (Okayama, Japan). The existence of a complete solid solution between stronalsite and banalsite was confirmed by Koneva (1996) in samples from the Zhidoy massif (Eastern Sayan, SE Russia). Tectosilicates of the stronalsite–banalsite series occurred there in feldspar–zeolite veins penetrating alkali pyroxenites at the contact with nepheline syenite. Most of known stronalsite occurrences are related to nepheline syenites of the Kola Alkaline Province (NW Russia). Khomyakov *et al.* (1990) studied botryoidal aggregates of stronalsite enclosed by a Na-Sr-rich melilite in a strongly altered xenolith of a cuspidine–melilite rock hosted by nepheline syenite of the Khibina peralkaline complex. Similarly, Dunworth and Bell (2003) identified stronalsite in the cuspidine-bearing nepheline melilitolite at the Turiy Mys complex of ultramafic–alkaline rocks and carbonatites. Liferovich *et al.* (2006b) re-examined xenolith samples from Khibina and interpreted stronalsite from both occurrences to be a metasomatic phase formed by a relatively high-temperature alteration of Na-Sr-rich melilite and/or nepheline. Liferovich *et al.* (2006b) also described three new occurrences from the Kola Alkaline Province: in leucocratic ijolite cut by calciocarbonatite and banded phoscorite at the Turiy Mys ultramafic–alkaline complex, in coarse-grained urtite at the Gremyakha-Vyrmes complex of mafic–ultramafic rock, quartz syenites and feldspathoid rocks, and in medium-grained essexite xenolith in a

nepheline syenite at the Sakharjok alkaline massif. In addition, Liferovich *et al.* (2006b) described paragenesis and composition of stronalsite, banalsite and their intermediate compositional members from feldspathoid syenites of the Pilansberg peralkaline complex in South Africa, and from xenoliths of apatite–calcite-bearing stronalsite clinopyroxenite to serpentine–calcite mylonite and diverse rocks of ijolite series at the Prairie Lake complex of alkaline rocks and carbonatites in the Superior Alkaline Province (NW Ontario, Canada). Another occurrence of stronalsite was described by Ahijado *et al.* (2005) from metasomatic calc-silicate reaction zones in skarn associated with metamorphosed carbonatites at Punta del Peñón Blanco area (Fuerteventura, Canary Islands, Spain). Sporadic occurrences of stronalsite–banalsite have been reported also from the Late Archean Mikkelvik alkaline stock in the West Troms Basement Complex (Zozulya *et al.*, 2009), and from amygdules in alkaline ultramafic rocks of the Brunlanes ultramafic volcanic series (Dahlgren and Larsen, 2012), both in Norway. Finally, Ferraris *et al.* (2014) identified stronalsite and banalsite in mineral association with trinepheline and fabrièsite in nephelinitic-albitic jadeitite from the metamorphic veins of the Tawmaw-Hpakant jadeite deposit (Myanmar).

This work deals with the first occurrence of stronalsite in the rocks of the teschenite association in the Silesian Unit (Flysch Belt of the Western Carpathians, Czech Republic). Two compositionally different types of stronalsite were identified in pseudomorphs after an unknown phenocrystic mineral in Sr-enriched hydrothermally altered dykes of leucocratic teschenite, consisting dominantly of alkali feldspar and zeolites. The first type is a common Ca-poor member of the stronalsite–banalsite solid-solution series, while the second one has an unusual Ca-enriched composition. We discuss possible substitution mechanisms and try to clarify the origin of studied stronalsite based on mineral paragenesis and chemical and Sr-isotopic composition.

Geological background

The teschenite association is represented by mostly alkaline magmatic rocks (geochemical equivalents of alkaline basalts, basanites, and nephelinites) and ultrabasic picrites (e.g., Kudělásková, 1987; Hovorka and Spišiak, 1988; Safai, 2020). The term teschenite is defined in the sense of the IUGS petrographic classification (Le Maitre *et al.*, 2002) as analcime gabbro, but the classification of rocks of the teschenite association is difficult due to their large variability in mineral composition, different structural and textural features and strong hydrothermal alteration (analcimization, chloritization, smectitization, and carbonatization; e.g., Kapusta and Włodyka, 1997; Pour *et al.*, 2022; Rapprich *et al.*, 2024). For these reasons, the term teschenite was used for various types of hydrothermally altered foid syenite, foid monzosyenite, foid monzogabbro, foid gabbro and alkaline lamprophyres (e.g., Pacák, 1926; Šmíd, 1978; Kudělásková, 1987; Hovorka and Spišiak, 1988; Dostal and Owen, 1998; Rapprich *et al.*, 2024), which typically occur in the northern foothills of the Beskydy Mountains between towns of Hranice in Czech Republic and Bielsko-Biała in Poland (e.g., Hovorka and Spišiak, 1988). This area is a part of the Silesian Unit (Flysch Belt of the Outer Western Carpathians), which is a remnant of an external sedimentary basin developed on the southern margin of the European Platform (Nemčok *et al.*, 2001) and later incorporated into the Carpathian accretion wedge during the Alpine orogeny (Plašienka, 1997; Froitzheim *et al.*, 2008; Stráník *et al.*, 2021). The alkaline magmatism was associated with early rifting (Narebski, 1990; Spišiak and Hovorka, 1997; Brunarska and Anczkiewicz, 2019) or with reactivation of deep faults within the basin during the Lower Cretaceous (Dostal and Owen, 1998). The ^{40}K-^{40}Ar and ^{39}Ar-^{40}Ar whole-rock dating of the teschenites and in-situ mineral U-Pb dating reveals age of ~138–120 Ma (Lucińska-Anczkiewicz *et al.*, 2002;

Grabowski *et al.*, 2003; Szopa *et al.*, 2014; Matýsek *et al.*, 2018; Brunarska and Anczkiewicz, 2019). Magmatic activity was coeval with deposition of the Hradiště Fm. (Valanginian-Aptian; Eliáš *et al.*, 2003; Stráník *et al.*, 2021). Lithology of the Hradiště Fm. includes typical flysch sediments (various types of grey calcareous claystones, sandy limestones and sandstones), dark organic silicites, pelocarbonates, and bodies of igneous rocks of the teschenite association (mostly hypabyssal sills, submarine extrusions, pillow lavas and volcanoclastics; Stráník *et al.*, 1993, 2021). The intrusions also penetrated the underlying calcareous sediments, represented by deep-water dark brown-grey calcareous claystones of the Vendryně Fm. (Oxfordian-Tithonian; Eliáš, 1970; Menčík *et al.*, 1983) and micritic or biodetritic Těšín limestone (Tithonian-Valanginian; Eliáš, 1970; Stráník *et al.*, 2021). Trace element contents and the Nd, Sr, and Hf isotopic composition indicate that the magma was probably a product of ~2–6 % partial melting of upper mantle garnet peridotite at ~60–80 km depth. Geochemical studies also suggest compositional similarities to ocean island basalts (OIB) with HIMU affinities and possible mixing with a more depleted, MORB-type component (Dostal and Owen, 1998; Harangi *et al.*, 2003; Brunarska and Anczkiewicz, 2019).

Occurrence and paragenesis

The Čerťák (or "Čertův mlýn") occurrence (49°33'58"N, 17°59'54"E) represents a well-known surface exposure of a teschenite sill ca. 2 km south from the town of Nový Jičín. This sill runs in the SW–NE direction in a total length exceeding 2 km (Fig. 2) and is composed of various petrographic types of teschenitic rocks. The dominant type is hydrothermally altered mesocratic teschenite, which is coarse-grained to porphyritic and consists of phenocrysts of black prismatic clinopyroxene and amphibole (up to 3.5 cm long) and a grey-pinkish

groundmass composed of feldspars, zeolites, biotite, apatite and other accessory or secondary minerals (e.g., Pacák, 1926; Šmíd, 1978; Kudělásková, 1987; Hovorka and Spišiak, 1988; Matýsek and Jirásek, 2016; Kropáč *et al.*, 2020, 2024). Less abundant are melanocratic pyroxene-rich varieties or, conversely, leucocratic varieties that, before being altered by hydrothermal fluids, often had a nepheline-rich composition (e.g., Pacák, 1926). They form up to several cm thick fine- to medium-grained dykes, streaks or nests randomly distributed in the mesocratic teschenite. The mineral association of leucocratic teschenites from the Čerťák occurrence was recently studied in detail by Matýsek and Jirásek (2016) and Kropáč *et al.* (2020, 2024). Accurate classification of leucocratic teschenites is problematic due to a strong hydrothermal alteration. Matýsek and Jirásek (2016) compare these rocks to metasomatic rodingites, but this suffers due to a lack of association with serpentinite bodies. The rock consists of subhedral lamellae or anhedral irregular grains of alkali feldspar (Na-rich microcline with ~0.30 apfu Na), celsian (≤0.21 apfu Sr) and slawsonite (≤0.91 apfu Sr; Matýsek and Jirásek, 2016). Primary calcic plagioclase is not preserved due to hydrothermal alteration, which began immediately after solidification (Kropáč *et al.*, 2020). Plagioclase was probably replaced by analcime, natrolite, and Sr-rich thomsonite-Ca, or, alternatively, by albite, K-feldspar and epidote-(Sr) to Sr-rich epidote (Kropáč *et al.*, 2024). Slawsonite is intergrown with mica minerals of the muscovite (illite)–paragonite series (Matýsek and Jirásek, 2016). Mafic components are represented by sporadic euhedral prismatic phenocrysts of clinopyroxene (Ti-rich diopside rimmed by hedenbergite or aegirine-augite to aegirine) and amphibole (kaersutite or ferrokaersutite with hastingsite or ferropargasite rim) and leaflets of biotite (annite). The rock association is completed by accessory minerals (fluorapatite, REE-rich fluorapatite, Ti-rich magnetite, (OH, F)-rich grossular, epidote-(Sr), Sr-REE-rich epidote, Sr-rich allanite-(Ce), Zr-Nb-rich titanite, pyrochlore, zircon, and vesuvianite), prehnite, chlorite (chamosite), pyrite, calcite and baryte (Kropáč *et al.*, 2020, 2024).

Methods

We re-examined a total of 11 samples of leucocratic dykes, streaks or nests from the Čerťák locality, which were recently studied by Kropáč *et al.* (2020, 2024). Only two samples (Č7 and Č10), which were found to contain stronalsite, were selected for a detailed study. Electron microprobe analyses were performed using Cameca SX-100 apparatus at the National Museum in Prague, Czech Republic (Z. Dolníček analyst). The measurements were carried out on carbon-coated polished thin sections in a wavelength-dispersive mode. The detection limits, acceleration voltage, beam current and diameter, analytical lines, standards and diffracting crystals are specified in Supplementary Tables S1–S5, which include all analyses of the studied tectosilicates. Non-stoichiometric analyses of the feldspar-muscovite or the Na-Ca zeolite mixtures were omitted. The raw counts were converted to wt. % using the automatic PAP procedure (Pouchou and Pichoir, 1985). Mineral abbreviations are according to Warr (2021).

In situ micro-Raman analyses of minerals were performed using a DXR dispersive Raman Spectrometer mounted on a confocal Olympus microscope housed in the National Museum in Prague, Czech Republic. The Raman signal was excited by an unpolarised 633 nm laser and detected by a CCD detector. The spectrometer was calibrated using a software-driven procedure based on emission lines of neone (calibration of Raman shift), Raman bands of polystyrene (calibration of laser frequency) and standardized source of white light (calibration of intensity). The parameters of measurement were 100× objective, 5 s exposure time, 100 exposures, 50 μm pinhole spectrograph aperture, 8 mW laser power, and 40–3700 cm^{-1} spectral range. Spectral manipulations were performed using the Omnic 9 software.

Results

Stronalsite bearing mineral association

Stronalsite occurs as a constituent of columnar, rectangular or hexagonal skeletal pseudomorphs in hydrothermally altered leucocratic dykes or streaks. These pseudomorphs are randomly distributed in medium- to coarse-grained parts close the boundary with the host mesocratic amphibole-pyroxene teschenite (Figs. 3a,b). The mineral association in the vicinity of pseudomorphs (Figs. 3c,d) consists mostly of euhedral to subhedral slats of alkali feldspars, anhedral natrolite, thomsonite-Ca and rarely also analcime, columns of amphibole, leaflets of chloritized biotite, needles or hexagonal skeletal crystals of fluorapatite and other accessory and/or secondary minerals (epidote group minerals, titanite, pyrochlore, Ti-rich magnetite, chlorite, prehnite, pyrite, calcite and baryte). Stronalsite forms anhedral colourless grains (Fig. 3e) with low birefringence. Some grains are corroded by zeolites and/or muscovite. In rare case, where both Ba- and Ca-rich stronalsite occurs together within a single pseudomorph, the Ba-rich stronalsite is clouded by products of hydrothermal alteration, whereas Ca-rich stronalsite is relatively well preserved (Fig. 3f). The paragenetic relationships are more obvious in the BSE images (Figs. 4a–c and Figs. 5a,b). Based on results of WDS analysis and Raman spectroscopy, both Ca- and Ba-rich stronalsite are replaced along rims and subparallel cracks by natrolite, thomsonite-Ca, muscovite and their mixture, similarly to slawsonite. In addition, a small amount of anhedral K-feldspar and tiny euhedral to anhedral grains of celsian may occur in this hydrothermal association (Fig. 4a). If they occur in a single pseudomorph, the Ba-rich stronalsite overgrows slawsonite, which must have crystallized earlier (Fig. 4b). The Ca-rich stronalsite appears relatively more homogenous in a BSE image. It also rarely forms a marginal zone on hydrothermally altered Ba-rich stronalsite inside the

hexagonal skeletal pseudomorph (Fig. 4c) and is thus younger. The "atoll" itself consists only of slawsonite and a Na-Ca zeolite-muscovite mixture (Fig. 4c). Some "atolls" have been completely replaced by prehnite, which also fills cracks and cavities in rock and is therefore younger. Most hexagonal skeletal pseudomorphs, although rather frequent in the rock, do not contain stronalsite. Their central part is usually filled with subhedral to anhedral titanite, epidote, hedenbergite, alkali feldspars and Na-Ca zeolites (Fig. 4d).

Raman spectroscopy

Raman spectroscopy confirmed the presence of natrolite, thomsonite-Ca, muscovite, slawsonite and stronalsite in the studied pseudomorphs. Raman spectra of chemically different types of stronalsite were also measured in rectangular pseudomorphs (sample Č10). The peak position of both Ba- and Ca-rich stronalsite varieties are practically identical (Figs. 5a,b).

Chemical composition

The representative chemical composition of stronalsite is shown in Table 1 (all analyses are available in Table S1). Most of the analyzed stronalsite represents typical members of the stronalsite–banalsite solid-solution series. The Ba-rich stronalsite is characterized by high contents of Sr (0.55–0.83 apfu) and subordinate contents of Ba (0.12–0.37 apfu) and/or Ca (0.00–0.08 apfu) (Tables 1 and S1, Figs. 6a–c). Only sample Č10 included also stronalsite rich in Ca, which contains 0.65–0.82 apfu Sr, 0.10–0.23 apfu Ca and only 0.01–0.06 apfu Ba (Tables 1 and S1, Figs. 6a–c). The Na contents vary in a wide range 1.82–2.42 apfu, while the

K contents are mostly negligible (0.00–0.09 apfu). The poor stoichiometry in the *Na* site in some analyses can be explained mainly by issues in the determination of Na by electron microprobe. Similar problems with the estimation of Na in stronalsite were pointed out by several authors (e.g., Matsubara, 1985; Khomyakov *et al.*, 1990; Koneva, 1996; Liferovich *et al.*, 2006b). The *T* site contains 3.91–4.26 apfu Si, 3.76–4.00 apfu Al and 0.00–0.11 apfu Fe^{3+} (Table S1).

The chemical composition of slawsonite is variable ($Sws_{49–83}Cls_{4–19}Or_{1–12}Ab_{2–22}An_{1–8}$; Fig. 6d, Table S2). The Sr and Ba contents range 0.51–0.93 and 0.04–0.24 apfu, respectively. Most celsian grains are close to its near-ideal chemical composition ($Cls_{93–99}$; Fig. 6d, Table S3). Alkali feldspars chemically correspond to K-feldspar ($Or_{88–98}Ab_{1–7}An_{0–2}Sws_{0–2}Cls_{0–3}$) or to a K-feldspar with a significant portion of albite component ($Or_{64–73}Ab_{26–32}An_{1–2}Sws_{0–1}$) (Fig. 6e, Table S4). Both types form mostly irregular zones in feldspar grains, or in some cases, the Na-poor K-feldspar overgrows the Na-rich core. In addition, some K-feldspars show growth zonation due to enrichment in Ba ($Cls_{7–10}$; brighter in BSE in Fig. 5a,b). The chemical composition of zeolites illustrates Table S5. Only one analysis was performed in analcime due to its rare occurrence in the studied samples. Its composition is close to ideal stoichiometry. This also applies to the more frequently present natrolite. The contents of Fe, Mg, Ca and K in natrolite are close or below the detection limit. In contrast, thomsonite-Ca shows variable contents of Ca (1.22–1.90 apfu) and Sr (0.14–0.73 apfu) (Table S5). This variability is not dependent on position within the sample (pseudomorphs or groundmass).

Discussion

Crystal chemistry of stronalsite

The chemical composition of Ba-rich stronalsite from the Čerťák locality mostly fits well the composition of minerals of the stronalsite–banalsite solid-solution series described by Liferovich *et al.* (2006b). Similar Ba-rich composition shows certain analyses from Prairie Lake, Sakhorjok or Gremyakha-Vyrmes occurrences (see Liferovich *et al.*, 2006b). On the other hand, our analyses do not approximate the end-member composition represented by stronalsite from the Khibina occurrence (Figs. 6a–c). In contrast, Ca-rich stronalsite is extremely rare worldwide. So far, the highest content of Ca in stronalsite reported the analysis from the Gremyakha-Vyrmes occurrence (1.4 wt. % CaO, i.e., 0.15 apfu Ca; Liferovich *et al.* 2006b). Stronalsite from sample Č10, however, contains up to 2.2 wt. % CaO (i.e., 0.23 apfu Ca; Tables 1 and S1; Figs. 6a–c).

Three substitution mechanisms explaining the incorporation of Ca into the stronalsite structure can be suggested. The first one involves the entrance of Ca to the *A* position of the ideal formula, i.e., substituting divalent cations (Sr, Ba). This approach would theoretically suggest the presence of up to ~25 mol. % of the lisetite component, if miscibility with banalsite–stronalsite would exist (Tables 1 and S1; Figs. 6a–c). Stoichiometric criteria of our WDS analyses strongly support this possibility: the sum of cations in *A* position (i.e., Sr + Ba + Ca) are then close to the ideal value of 1 apfu (average 0.96, range 0.89–1.04; Table S1) for Ca-rich compositions. However, the formation of a solid solution between banalsite–stronalsite and lisetite would be hampered by differences in their crystal structures (Liferovich *et al.*, 2006a,b). In the first case, the Ba or Sr and Na cations are ordered, and populate alternating layers parallel to (001), separated by ¼ *c*, whereas in lisetite Ca and Na cations are distributed throughout common Ca + 2Na layers (Figs. 1a,b; Rossi *et al.*, 1986; Liferovich *et al.*, 2006a). Although data plotted in Fig. 7a suggest that there is no evidence of a $(Sr,Ba)^{2+} \leftrightarrow Ca^{2+}$ substitution ($R^2 = 0.50$), relatively narrow range of compositions (Ca contents cover

range over 0.23 apfu for the whole dataset) in combination with a comparably wide scatter of the total *A*-site occupancy (within 0.19 apfu) likely influenced the scattering of data points.

Second, the incorporation of Ca could also be realized in *Na* position of the ideal formula. Replacing Na for Ca would solve the above-mentioned crystal-structure limitations. However, such an approach results in a strong deficit in the *A* position (average 0.77, range 0.70–0.87 apfu Sr + Ba) and mostly significant excess of atoms in *Na* position (average 2.24, range 2.01–2.45 apfu Na + K + Ca) for Ca-rich compositions. The latter, however, can be potentially caused by problems with Na determinations using an electron microprobe. Moreover, the heterovalent $Na^{+} \leftrightarrow Ca^{2+}$ substitution would be coupled with $Si^{4+} \leftrightarrow (Al, Fe)^{3+}$ substitution in order to obtain an electroneutral substitution vector: $Si^{4+} + Na^{+} \leftrightarrow Al^{3+} + Ca^{2+}$ (Fig. 7b). However, no correlations are obtained for this coupled substitution ($R^2 = 0.44$) as well as for simple pairs Ca-Si or Ca-$(Al, Fe)^{3+}$ ($R^2 \leq 0.04$; Figs. 7c,d).

The third possibility is a modification of the second one. In the absence of substitutions involving the tetrahedral site, the electroneutrality can also be achieved by a coupled heterovalent substitution comprising *A* and *Na* positions: $^{Na}Na^{+} + {}^{A}Sr^{2+} \leftrightarrow {}^{A}Na^{+} + {}^{Na}Ca^{2+}$. Regarding the difficulties with Na analysis, this mechanism could be easily verified due to the existence of a correlation between "vacancy" in *A* position (expressed as a sum of Sr and Ba) and Ca contents. However, such a correlation is not evident ($R^2 = 0.50$; Fig. 7a).

It can be concluded that, at the present state of knowledge, the role of Ca in the stronalsite formula cannot be specified unambiguously. This is due to common analytical limitations and also due to the studied material, which covers a narrow range of compositions only (within ca. 0.15 apfu in case of Ca-rich stronalsite). Future studies are necessary to constrain this task adequately. Nevertheless, the entry of an elevated amount of Ca into the structure of

stronalsite did not apparently cause its significant deformation, which is documented by identical Raman spectra of both Ca-rich and Ca-poor varieties (Figs. 5a,b).

The source of strontium

The source of Sr was specified based on a comparison of the $^{87}Sr/^{86}Sr_{i(120\ Ma)}$ isotopic ratio of the studied Sr-rich leucocratic teschenites (samples Č7 and Č10) with different rock types of the teschenite association, Upper Jurassic-Lower Cretaceous sediments of the Silesian Unit and Lower Cretaceous seawater (Kropáč *et al.*, 2024). This isotopic study confirmed earlier evidence (Dolníček *et al.* 2010a,b; Kropáč *et al.*, 2017), which clearly showed that Sr isotope composition must have been modified during post-magmatic interaction with fluids of an external origin. The leucocratic dykes Č7 and Č10 have slightly higher $^{87}Sr/^{86}Sr_{i(120\ Ma)}$ ratios (0.7047 and 0.7046, respectively) than other members of the teschenite association including the host mesocratic teschenite from the Čerťák site ($^{87}Sr/^{86}Sr_{i(120\ Ma)}$ = 0.7045 and 0.7038) and significantly lower $^{87}Sr/^{86}Sr_{i(120\ Ma)}$ ratios when compared to Upper Jurassic-Lower Cretaceous sediments of the Silesian Unit ($^{87}Sr/^{86}Sr_{i(120\ Ma)}$ = 0.7073–0.7083; Kropáč *et al.*, 2024) and Lower Cretaceous seawater ($^{87}Sr/^{86}Sr$ = 0.7071–0.7075; Veizer *et al.*, 1999). Based on the mass balance, Kropáč *et al.* (2024) calculated a contribution of at least 6–17 % Sr from the surrounding claystones of the Hradiště Fm. (if the system claystone–host teschenite is considered) or 8–21 % Sr from Lower Cretaceous seawater (if the system seawater–host teschenite was inferred). The primary magmatic intermediate plagioclase was probably the main source of Sr, even though it was not preserved at the Čerťák locality. Tabular relics of andesine–labradorite ($An_{36–52}$) with up to 0.44–0.57 wt. % SrO were described from leucocratic dykes at the Řepiště occurrence in the Silesian Unit (Kropáč *et al.*, 2020, 2024).

The genesis of stronalsite

Large amounts of alkali- and Sr-Ba-bearing tectosilicates in the studied pseudomorphs testify to the complex genesis of the mineral association, which involved the participation of both late-magmatic and hydrothermal processes. Reconstruction of the magmatic evolution is difficult due to intense superimposed hydrothermal alteration. The teschenite magma in the late stage already carried sporadic phenocrysts of apatite, pyroxene and amphibole. The Sr-enriched plagioclase, nepheline and alkali feldspar also crystallized from the felsic melt. After the sill intruded into the water-saturated unconsolidated seafloor sediments, the residual melt rapidly cooled and solidified, probably in the form of a glassy groundmass (Pour *et al*., 2022; Rapprich *et al.*, 2024). The end of the late-magmatic phase was associated with autometamorphic (autometasomatic) processes, which were triggered by high-temperature magmatic brines interacting with fluids of an external origin (Dolníček *et al.*, 2010a,b; Kropáč *et al.*, 2017, 2024; Rapprich *et al.*, 2024).

Clarifying the relationships between Sr-, Ba- and alkali feldspars is essential for resolving the genesis of stronalsite. According to Matýsek and Jirásek (2016), slawsonite crystallized in autometamorphic phase together with celsian and Na-K feldspar ($Ab_{20–40}$). However, K-feldspar with ~30 mol. % of the Ab component crystallizes in igneous systems usually at temperatures significantly higher than ~600 °C. The existence of a Na-rich homogeneous crystal below this temperature is limited by the miscibility gap (e.g., Brown and Parsons, 1989). We therefore consider the Na-K-feldspar associated with pseudomorphs to be a product of crystallization from a melt that corroded phenocrysts in the late stage of magmatic evolution. Alternatively, an inclusion of melt trapped in a growing phenocryst cannot be excluded, as is evidenced by Kropáč *et al.* (2015). But could Ba and Sr feldspars have formed

from the melt under the same conditions? This is not indicated by textural features that point to a hydrothermal origin, nor by the fact that apparently primary magmatic minerals, such as apatite or calcic plagioclase, did not show a trend of gradually increasing Sr contents during crystallization (Kropáč *et al.*, 2024). Therefore, we suggest that the Ba-Sr phases crystallized under subsolidus conditions after the system was opened to seawater, which is also supported by the Sr isotopic composition (Kropáč *et al.*, 2024).

The hydrothermal alteration of Sr-bearing plagioclase probably started already during high-temperature autometasomatic stage and continued into the hydrothermal stage. The formation of Sr-absent secondary minerals, such as analcime, K-feldspar or albite, during the decomposition of calcic plagioclase resulted in increased Sr concentrations in the hydrothermal solution (Kropáč *et al.*, 2024). Stronalsite could only crystallize under silica-poor conditions, because a slight increase in Si would instead favor the formation of slawsonite (Matsubara, 1985; Hori *et al.*, 1987). Since slawsonite is successively older than stronalsite, we can assume higher Si concentrations at the initial phase of Sr-feldspar crystallization, reflecting the hydrothermal breakdown of primary silicates and glassy groundmass. The Sr/Ba ratio in the hydrothermal solution was probably influenced by celsian precipitation. The formation of Ca-rich stronalsite may be related to the depletion of Ba ions after the crystallization of celsian.

Crystallization mechanisms

The genesis of minerals of stronalsite–banalsite series in altered alkaline rocks was discussed by Liferovich *et al.* (2006b). Based on the textural relationships between primary nepheline and analcime-rich secondary assemblage, these authors interpreted stronalsite to be mostly a

product of nepheline replacement during subsolidus reaction with a deuteric alkaline fluid. They schematically expressed this reaction as follows:

$$2Na_3KAl_4Si_4O_{16} + 2SrO + Al_2O_3 + 4SiO_2 + 2H_2O \rightarrow 2SrNa_2Al_4Si_4O_{16} + 2NaAlSi_2O_6 \cdot H_2O + K_2O. \quad (1)$$

Nepheline was probably abundant primary mineral in leucocratic teschenites, as is indicated by numerous hexagonal pseudomorphs (Pacák, 1926). Matýsek and Jirásek (2016) also favour nepheline (and less likely also plagioclase) as a precursor for slawsonite pseudomorphs. Therefore, stronalsite in the studied rocks could have crystallized at the expense of nepheline. Unlike the mineral associations studied by Liferovich *et al.* (2006b), analcime is relatively rare in leucocratic teschenites with originally nepheline-rich composition (e.g., Pacák, 1926). Šmíd (1978) noted that secondary analcime replaces alkali feldspars or less plagioclase in teschenites, but never nepheline. However, the low amount of analcime can be possibly explained by intense natrolitization during the late hydrothermal alteration.

Liferovich *et al.* (2006b) also noted that under specific physico-chemical conditions, hydrothermal alteration of nepheline can also lead to the crystallization of stronalsite and albite instead of analcime:

$$2Na_3KAl_4Si_4O_{16} + 2SrO + Al_2O_3 + 6SiO_2 \rightarrow 2SrNa_2Al_4Si_4O_{16} + 2NaAlSi_3O_8 + K_2O. \quad (2)$$

Although albite was identified together with K-feldspar and epidote-(Sr) in the pseudomorphs, possibly after plagioclase, in the studied samples (Kropáč *et al.*, 2024), it was never observed in the stronalsite-bearing pseudomorphs, making this explanation improbable.

The K released during hydrothermal reactions could subsequently be incorporated into the structure of late K-feldspar and mica (Liferovich *et al.*, 2006b). An alternative possibility may

be that the K-feldspar and muscovite were produced together with stronalsite during hydrothermal alteration of nepheline associated with slawsonite:

$$2Na_3KAl_4Si_4O_{16} + 3SrAl_2Si_2O_8 + 4SiO_2 \rightarrow 3SrNa_2Al_4Si_4O_{16} + 2KAlSi_3O_8, \quad (3)$$

and

$$2Na_3KAl_4Si_4O_{16} + SrAl_2Si_2O_8 + 2H_2O \rightarrow SrNa_2Al_4Si_4O_{16} + 2KAl_2(AlSi_3O_{10})(OH)_2 + 2Na_2O. \quad (4)$$

The breakdown product of nepheline and associated slawsonite could theoretically also be K-feldspar and natrolite, together with stronalsite:

$$2Na_3KAl_4Si_4O_{16} + SrAl_2Si_2O_8 + 6SiO_2 + 4H_2O \rightarrow SrNa_2Al_4Si_4O_{16} + 2KAlSi_3O_8 + 2Na_2Al_2Si_3O_{10} \cdot 2H_2O. \quad (5)$$

The coeval genesis of stronalsite, K-feldspar and natrolite seems problematic because natrolite postdates the feldspars, as is clearly evidenced by textural features. Natrolite fills fractures in stronalsite and occurs in intimate mixtures with thomsonite-Ca, indicating very low crystallization temperatures (Kristmanndóttir and Tómasson, 1978). Thomsonite-Ca additionally contains up to 0.73 apfu Sr, which may have been released from hydrothermally altered stronalsite and slawsonite.

Considering that the system was most probably opened during the hydrothermal alteration of the rock, it is necessary to take all suggested mechanisms with caution. Hydrothermal decomposition of the glassy groundmass could enrich the deuteric fluids in Na (Rapprich *et al.*, 2024) and the contribution of other ions by mixing with external fluids should also be considered (Dolníček *et al.*, 2010a,b; Kropáč *et al.*, 2020, 2024).

Crystallization conditions

Since stronalsite is probably younger than slawsonite and crystallized with analcime before the formation of natrolite and thomsonite-Ca, we can at least indirectly estimate the conditions of its crystallization. Liebscher *et al.* (2009) synthesized slawsonite and other Ca-Sr-phases from oxide-hydroxide-fluid mixture at a temperature of 400–500 °C and a pressure of 390–500 MPa. However, in natural systems, slawsonite can crystallize under even lower P-T conditions, as evidenced by Tasáryová *et al.* (2014). These authors studied slawsonite in mineral association with celsian and hyalophane in picrites from the Upper Ordovician strata of the Prague Basin, Czech Republic. Tasáryová *et al.* (2014) concluded that Sr- and Ba-feldspars precipitated directly from a fluid phase, which caused decomposition of calcic plagioclase at T ≤350 °C and P <500 MPa.

According to Liou (1971), analcimization of nepheline probably occurred at temperatures below 450 °C. Based on the model for autometasomatic alteration of sodic peralkaline rocks according to Marks and Markl (2003), Liferovich *et al.* (2006b) estimated the conditions for the conversion of nepheline to analcime at temperatures below 300 °C, H_2O activities between 0.5 and 1.0, and oxygen fugacity above the magnetite–hematite buffer. These conditions can also be applied to our case. A higher oxygen fugacity is evidenced by the presence of aegirine-augite or aegirine and Sr-rich minerals of the epidote group, which crystallized from hydrothermal solutions probably at pressures below 100 MPa and at ~250–430 °C (Kropáč *et al.*, 2024), based on the chlorite thermometry (~250–310 °C) and fluid inclusion studies from other occurrences of teschenites in the Silesian Unit (Dolníček *et al.*, 2010a). The homogenization temperatures of primary and pseudosecondary fluid inclusions in analcime from miaroles, amygdules and veins hosted by rocks of the teschenite association range between 100 and 320 °C and trapped aqueous fluids have low salinity of 0.5–4.5 wt. %

NaCl equiv. (Włodyka and Kozlowski, 1997; Urubek *et al.*, 2013). Although these microthermometric data were not obtained from samples under this study, they may serve as important clues for approximating the origin of stronalsite. The temperature conditions of analcime crystallization may overlap to some extent with natrolite crystallization, which are likely younger than the studied stronalsite. The genesis of natrolite is generally associated with volatile-rich fluids and lower-temperature environment and its crystallization occurs usually at T <200 °C (Senderov and Khitarov, 1971). The same applies to minerals from the thomsonite subgroup. For instance, Kristmanndóttir and Tómasson (1978) determined the crystallization temperature of natrolite and thomsonite from Iceland geothermal fields to be even less than 100 °C.

Therefore, stronalsite in the studied rocks could crystallize in a relatively wider range of temperature conditions. The presence of Sr-enriched high- to medium-temperature hydrothermal fluids is evidenced by the crystallization of rare epidote-(Sr) at T ~250–430 °C (Kropáč *et al.*, 2024). In contrast, the Sr-rich thomsonite-Ca represents most probably late-hydrothermal redeposition of Sr from alteration of Sr feldspars at T <100 °C. Taken together with microthemometric data from analcime (Włodyka and Kozlowski, 1997; Urubek *et al.*, 2013), we can estimate the conditions for crystallization of stronalsite in the studied pseudomorphs at temperatures ~250–320 °C and pressures not exceeding 100 MPa.

Conclusion

The studied stronalsite represents the first occurrence of this rare Sr tectosilicate in the rocks of the teschenite association in the Silesian Unit, and, at the same time, in the Western Carpathians. Two compositionally distinct types have been described in leucocratic

teschenites: Ba-rich stronalsite and Ca-rich stronalsite. Both show identical Raman spectra. The substitution mechanism by which Ca ions enter the stronalsite structure cannot be unambiguously deciphered from the available data. Similar to older slawsonite, stronalsite was formed by hydrothermal alteration of phenocrysts (likely nepheline). In addition to both Sr tectosilicates, pseudomorphs also contain K-feldspar, celsian, natrolite, and thomsonite-Ca. The major source of Sr was probably primary magmatic plagioclase, which, like nepheline, was completely altered during hydrothermal alteration. Part of Sr could also be derived from fluids of external origin. The crystallization conditions are difficult to determine because both the pseudomorphs after felsic minerals and the groundmass were subject of intense zeolitization. Based on the textural relationships of minerals present in the studied pseudomorphs and comparison with earlier investigations, we suggest that stronalsite crystallized just between a high-temperature and a low-temperature hydrothermal stages, probably in a temperature range of ~250–320 °C at pressure <100 MPa.

Acknowledgments. This work was supported by the Palacký University Olomouc (IGA_PrF_2019_017) to K.K and by the Ministry of Culture of the Czech Republic (long-term project DKRVO 2024–2028/1.II.b; National Museum, 00023272) to Z.D. We also thank to three anonymous reviewers for constructive and helpful comments, which improved the clarity of the manuscript.

Electronic supplementary material. The electron microprobe analyses of stronalsite, slawsonite, celsian, alkali feldspars and zeolites are available online at the Journal website (*http://*....).

References

Ahijado A., Casillas R., Nagy G. and Fernández C. (2005) Sr-rich minerals in a carbonatite skarn, Fuerteventura, Canary Islands (Spain). *Mineralogy and Petrology*, **84**, 107–127. https://doi.org/10.1007/s00710-005-0074-8

Brown W.L. and Parsons I. (1989) Alkali feldspars: ordering rates, phase transformations and behaviour diagrams for igneous rocks. *Mineralogical Magazine*, **53**, 25–42.

Brunarska I. and Anczkiewicz R. (2019) Geochronology and Sr–Nd–Hf isotope constraints on the petrogenesis of teschenites from the type-locality in the Outer Western Carpathians. *Geologica Carpathica*, **70**, 222–240. https://doi.org/10.2478/geoca-2019-0013

Campbell Smith W., Bannister F.A. and Hey M.H. (1944a) A new Barium-feldspar from Wales. *Nature*, **154**, 336–337. https://doi.org/10.1038/154336c0

Campbell Smith W., Bannister F.A. and Hey M.H. (1944b) Banalsite, a new barium-feldspar from Wales. *Mineralogical Magazine*, **27**, 33–47. https://doi.org/10.1180/minmag.1944.027.186.01

Cháb J., Stráník Z., Eliáš M. (Eds.) Adamovič J., Aichler J., Babůrek J., Breiter K., Cajz V., Domečka K., Fišera M., Hanžl P., Holub V., Hradecký P., Chlupáč I., Klomínský J., Krejčí Z., Lexa J., Mašek J., Mlčoch B., Opletal M., Otava J., Pálenský P., Potfaj M., Prouza V., Roetzel R., Růžička M., Schovánek P., Slabý J., Valečka J. and Žáček V. (2007) Geological map of the Czech Republic 1:500 000, ČGS Prague.

Dahlgren S. and Larsen A.O. (2012) Minerals of the banalsite-stronalsite series in amygdules from the Brunlanes ultramafic volcanic series. *Norwegian Mining Museum*, **49**, 93–100.

Dolníček Z., Kropáč K., Uher P. and Polách M. (2010a) Mineralogical and geochemical evidence for multistage origin of mineral veins hosted by teschenites at Tichá, Outer Western Carpathians, Czech Republic. *Chemie der Erde*, **70**, 267–282.

Dolníček Z., Urubek T. and Kropáč K. (2010b): Post-magmatic hydrothermal mineralization associated with Cretaceous picrite (Outer Western Carpathians, Czech Republic): interaction between host rock and externally derived fluid. *Geologica Carpathica*, **61**, 327–339.

Dostal J. and Owen J.V. (1998) Cretaceous alkaline lamprophyres from northeastern Czech Republic: geochemistry and petrogenesis. *Geologische Rundschau*, **87**, 67–77. https://doi.org/10.1007/s005310050190

Dunworth E.A. and Bell K. (2003) The Turiy massif, Kola peninsula, Russia: mineral chemistry of an ultramafic-alkaline-carbonatite intrusion. *Mineralogical Magazine*, **67**, 3, 423–451. https://doi.org/10.1180/0026461036730109

Eliáš M. (1970) Lithology and sedimentology of the Silesian Unit in the Moravskoslezské Beskydy Mts. *Sborník geologických věd, Řada Geologie*, **18**, 7–99 [in Czech].

Eliáš M., Skupien P. and Vašíček Z. (2003) A proposal for the modification of the lithostratigraphical division of the lower part of the Silesian Unit in the Czech area (Outer Western Carpathians). *Sborník vědeckých prací Vysoké školy báňské – Technické univerzity Ostrava, Řada hornicko-geologická*, **49**, 7–15 [in Czech].

Ferraris C., Parodi G.C., Pont S., Rondeau B. and Lorand J.-P. (2014) Trinepheline and fabriesite: two new mineral species from the jadeite deposit of Tawmaw (Myanmar). *European Journal of Mineralogy*, **26**, 257–265. https://doi.org/10.1127/0935-1221/2014/0026-2348

Froitzheim N., Plašienka D. and Schuster R. (2008) Alpine tectonics of the Alps and Western Carpathians. Pp. 1141–1232 in: *Geology of Central Europe 2: Mesozoic and Cenozoic* (T. McCann, editor). Bonn University, Germany. https://doi.org/10.1144/CEV2P.6

Grabowski J., Krzemiński L., Nescieruk P., Szydlo A., Paszkowski M., Pecskay Z. and Wójtowicz A. (2003) Geochronology of teschenitic intrusions in the Outer Western Carpathians of Poland–constraints from $^{40}K/^{40}Ar$ ages and biostratigraphy. *Geologica Carpathica*, **54**, 385–393.

Harangi S., Tonarini S., Vaselli O. and Manetti P. (2003) Geochemistry and petrogenesis of Early Cretaceous alkaline igneous rocks in Central Europe: implications for a long-lived EAR-type mantle component beneath Europe. *Acta Geologica Hungarica*, **46**, 77–94. https://doi.org/10.1556/AGeol.46.2003.1.6

Hori H., Nakai I., Nagashima K., Matsubara S. and Kato A. (1983) Unknown feldspar group mineral $SrNa_2Al_4Si_4O_{16}$ from Rendai, Kochi City. *Abstracts for Annual Meeting of the Mineralogical Society of Japan*, 10 [in Japanese].

Hori H., Nakai I., Nagashima K., Matsubara S. and Kato A. (1987) Stronalsite, $SrNa_2Al_4Si_4O_{16}$, a new mineral from Rendai, Kochi City, Japan. *Mineralogical Journal*, **13**, 368–375.

Hovorka D. and Spišiak J. (1988) *Mesozoic volcanism in the Western Carpathians*. Veda. Bratislava, 263 pp. [in Slovak].

Kapusta J. and Włodyka R. (1997) The X-ray powder analysis of analcimes from the teschenite sills of the Outer Carpathians, Poland. *Neues Jahrbuch für Mineralogie, Monatshefte*, **6**, 241–255.

Khomyakov A.P., Shpachenko A.K. and Polezhaeva L.I. (1990) Melilite and rare earth phosphate mineralization at the Namuaiv Mount (Khibina). Pp. 106–119 in: *Alkaline Magmatism at the NE part of the Baltic Shield* (T.N Ivanova, O.B Dudkin and A.A Arzamastsev, editors). Apatity, Kola Science Centre, Russian Academy of Sciences, Russia.

Koneva M.A. (1996) Banalsite and stronalsite from pyroxenites of the Zhidoy massif (the first Russian occurrence). *Zapiski Vserossiyskogo Mineralogicheskogo Obshchestva (Proceedings of Russian Mineralogical Society)*, **152**(2), 103–108 [in Russian].

Kropáč K., Dolníček Z., Buriánek D., Urubek T. and Mašek V. (2015) Carbonate inclusions in Lower Cretaceous picrites from the Hončova Hůrka Hill (Czech Republic, Outer Western Carpathians): Evidence for primary magmatic carbonates? *International Journal of Earth Sciences*, **104**, 1299–1315.

Kropáč K., Dolníček Z., Uher P. and Urubek T. (2017) Fluorcaphite from hydrothermally altered teschenite at Tichá, Outer Western Carpathians, Czech Republic: compositional variations and origin. *Mineralogical Magazine*, **81**, 1485–1501. https://doi.org/10.1180/minmag.2017.081.016

Kropáč K., Dolníček Z., Uher P., Buriánek D., Safai A. and Urubek T. (2020) Zirconian–niobian titanite and associated Zr-, Nb-, REE-rich accessory minerals: Products of hydrothermal overprint of leucocratic teschenites (Silesian Unit, Outer Western Carpathians, Czech Republic). *Geologica Carpathica*, **71**, 343–360. https://doi.org/10.31577/GeolCarp.71.4.4

Kropáč K., Dolníček Z., Uher P., Buriánek D. and Urubek T. (2024) Crystal chemistry and origin of epidote-(Sr) in alkaline rocks of the teschenite association (Silesian Unit,

Outer Western Carpathians, Czech Republic). *Mineralogy and Petrology*, **118**, 55–70. https://doi.org/10.1007/s00710-023-00847-w

Kristmanndóttir H., and Tómasson J. (1978) Zeolite zones in geothermal areas in Iceland. Pp. 277–284 in: *Natural zeolites, occurrence, properties, and use* (L.B Sand and F.A. Mumpton, editors). Pergamon, New York.

Kudělásková J. (1987) Petrology and geochemistry of selected rock types of teschenite association, Outer Western Carpathians. *Geologica Carpathica*, **38**, 545–573.

Le Maitre R.W., Ed. (2002) *Igneous Rocks: A Classification and Glossary of Terms*. Recommendations of the International Union of Geological Sciences Subcommission on the Systematics of Igneous Rocks, 2nd ed., 256 pp. Cambridge University Press.

Liebscher A., Thiele M., Franz G., Dörsam G. and Gottschalk M. (2009) Synthetic Sr-Ca margarite, anorthite and slawsonite solid solutions and solid-fluid Sr-Ca fractionation. *European Journal of Mineralogy*, **21**, 275–292. https://doi.org/10.1127/0935-1221/2009/0021-1917

Liferovich R.P., Mitchell R.H., Locock A. and Shpachenko A.K. (2006a) Crystal structure of stronalsite and a redetermination of the crystal structure of banalsite. *The Canadian Mineralogist*, **44**, 533–546.

Liferovich R.P., Mitchell R.H., Zotulya D.R. and Shpachenko A.K. (2006b) Paragenesis and composition of stronalsite, banalsite, and their solid solution in nepheline syenite and ultramafic alkaline rocks. *The Canadian Mineralogist*, **44**, 929–942.

Liou J.G. (1971) Analcime equilibria. *Lithos*, **4**, 389–402.

Lucińska-Anczkiewicz A., Villa I.M., Anczkiewicz R. and Ślaczka A. (2002) $^{40}Ar/^{39}Ar$ dating of alkaline lamprophyres from the Polish Western Carpathians. *Geologica Carpathica*, **53**, 45–52.

Marks M. and Markl G. (2003) Ilímaussaq "en miniature": closed-system fractionation in an agpaitic dyke rock from the Gardar Province, South Greenland. *Mineralogical Magazine*, **67**, 893–919.

Matsubara S. (1985) The mineralogical implication of barium and strontium silicates. *Bulletin National Science Museum, Tokyo Series C*, **11**, 37–95.

Matýsek D. and Jirásek J. (2016) Occurrences of slawsonite in rocks of the teschenite association in the Podbeskydí Piedmont area (Czech Republic) and their petrological significance. *The Canadian Mineralogist*, **54**, 1129–1146. https://doi.org/10.3749/canmin.1500101

Matýsek D., Jirásek K., Skupien P. and Thomson S.N. (2018) The Žermanice sill: new insights into the mineralogy, petrology, age, and origin of the teschenite association rocks in the Western Carpathians, Czech Republic. *International Journal of Earth Sciences*, **107**, 2553–2574.

Menčík E., Adamová M., Dvořák J., Dudek A., Jetel J., Jurková A., Hanzlíková E., Houša V., Peslová H., Rybářová L., Šmíd B., Šebesta J., Tyráček J. and Vašíček Z. (1983) *Geology of the Moravskoslezské Beskydy Mts. and the Sub-Beskidian Highland*. Ústřední Ústav geologický, Nakladatelství Československé akademie věd, Praha, 307 pp. [in Czech].

Nemčok M., Nemčok J., Wojtaszek M., Ludhova L., Oszczypko N., Sercombe W.J., Cieszkowski M., Paul Z., Coward M.P. and Ślaczka A. (2001) Reconstruction of Cretaceous rifts incorporated in the Outer West Carpathian wedge by balancing. *Marine and Petroleum Geology*, **18**, 39–64. https://doi.org/10.1016/S0264-8172(00)00045-3

Narebski W. (1990) Early rift stage in the evolution of western part of the Carpathians: geochemical evidence from limburgite and teschenite rock series. *Geologica Carpathica*, **41**, 521–528.

Pacák O. (1926) *Volcanic rocks at the northern foothill of the Moravské Beskydy Mts*. Česká Akademie Věd a Umění, Praha, 232 pp. [in Czech].

Plašienka D., Grecula P., Putiš M., Kováč M. and Hovorka D. (1997) Evolution and structure of the Western Carpathians: an overview. Pp. 1–24 in: *Geological Evolution of the Western Carpathians* (P. Grecula, D. Hovorka and M. Putiš, editors). Mineralia Slovaca Monograph, Bratislava.

Pouchou J.L. and Pichoir F. (1985) "PAP" (φpZ) procedure for improved quantitative microanalysis. Pp. 104–106 in: *Microbeam Analysis* (J.T. Armstrong, editor), San Francisco Press, San Francisco.

Pour O., Rapprich V., Matýsek D., and Jirásek J. (2022) About the origin of analcime in Meso- and Cenozoic volcanic rocks of the Czech Republic and its role in rock classification. *Geoscience Research Reports*, **55**, 75–81 [in Czech]. http://doi.org/10.3140/zpravy.geol.2022.10

Rapprich V., Matýsek D., Pour O., Jirásek J., Míková J. and Magna T. (2024) Interaction of seawater with (ultra)mafic alkaline rocks—Alternative process for the formation of aegirine. *American Mineralogist*, **109**, 488–501.

Rossi G., Oberti R. and Smith D.C. (1986) Crystal structure of lisetite, $CaNa_2Al_4Si_4O_{16}$. *American Mineralogist*, **71**, 1378–1383.

Safai A. (2020) *Distribution of selected high-field-strength elements in the rock of the teschenite association*. MSc Thesis, Palacký University Olomouc [in Czech].

Senderov E.E. and Khitarov N.I. (1971) Synthesis of thermodynamically stable zeolites in the Na_2O-Al_2O_3-SiO_2-H_2O. Pp. 149–154 in: *Molecular Sieve Zeolites-I* (M. Flanigen and L.B. Sand, editors). Advances in Chemistry Series, 101, American Chemical Society.

Spišiak J. and Hovorka D. (1997) Petrology of the Western Carpathians Cretaceous primitive alkaline volcanics. *Geologica Carpathica*, **48**, 113–121 [in Slovak].

Smith D.C., Kechid S.A. and Rossi G. (1986) Occurrence and properties of lisetite, $CaNa_2Al_4Si_4O_{16}$, a new tectosilicate in the system Ca-Na-Al-Si-O. *American Mineralogist*, **71**, 1372–1377.

Stráník Z., Menčík E., Eliáš M. and Adámek J. (1993) Flysch belt of the West Carpathians, autochthonous Mesozoic and Paleogene in Moravia and Silesia. Pp. 107–122 in: *Geology of Moravia and Silesia* (A. Přichystal, V. Obstová and M. Suk, editors). Moravské zemské muzeum, PřF MU, Brno [in Czech].

Stráník Z. (2021) Flysch belt. Pp. 95–234 in: *Geology of the Outer Western Carpathians and southeastern edge of the West European Platform in the Czech Republic* (Z. Stráník, M.

Bubík, H. Gilíková and P. Tomanová Petrová, editors). Czech Geological Survey, Prague [in Czech].

Szopa K., Włodyka R. and Chew D. (2014) LA-ICP-MS U-Pb apatite dating of Lower Cretaceous rocks from teschenite-picrite association in the Silesian Unit (southern Poland). *Geologica Carpathica*, **65**(4), 273–284. https://doi.org/10.2478/geoca-2014-0018

Šmíd B. (1978) *The investigation of igneous rocks of the teschenite association*. MS, Central Geological Survey, Prague, 153 pp. [in Czech].

Tasáryová Z., Frýda J., Janoušek V. and Racek M. (2014) Slawsonite-celsian-hyalophane assemblage from a picrite sill (Prague Basin, Czech Republic). *American Mineralogist*, **99**, 2272–2279.

Urubek T., Dolníček Z., Kropáč K. and Lehotský T. (2013) Fluid inclusions and chemical composition of analcimes from Řepiště (Outer Western Carpathians). *Geological Research in Moravia and Silesia*, **20**, 107–111 [in Czech].

Veizer J., Ala D., Azmy K., Bruckschen P., Bruhl D., Bruhn F., Carden G.A.F., Diener A., Ebneth S., Godderis Y., Jasper T., Korte Ch., Pawellek F., Podlaha O.G. and Strauss H. (1999) $^{87}Sr/^{86}Sr$, $\delta^{13}C$ and $\delta^{18}O$ evolution of Phanerozoic seawater. *Chemical Geology*, **161**, 59–88.

Warr L.N. (2021) IMA-CNMNC approved mineral symbols. *Mineralogical Magazine*, **85**, 291–320.

Włodyka R. and Kozlowski A. (1997) Fluid inclusions in hydrothermal analcimes from the rocks of the Cieszyn magma province (Poland). *ECROFI XIV Symposium*, 350–351.

Zozulya D., Kullerud K., Ravna E.K., Corfu F. and Savchenko Y. (2009) Geology, age and geochemical constraints on the origin of the Late Archean Mikkelvik alkaline stock, West Troms Basement Complex in Northern Norway. *Norwegian Journal of Geology*, **89**(4), 327–340.

Internet sources:

https://www.mindat.org/min-3804.html

https://www.mindat.org/min-2414.html

Fig. 1 Structures of $A Na_2Al_4Si_4O_{16}$ tectosilicates, a perspective views on unit cell along the *a* axis: (a) *Iba*2 structure of stronalsite [$SrNa_2Al_4Si_4O_{16}$] and banalsite [$BaNa_2Al_4Si_4O_{16}$] (modified after Liferovich *et al.*, 2006a and https://www.mindat.org/min-3804.html); (b) *Pbc*2_1 structure of lisetite [$CaNa_2Al_4Si_4O_{16}$] (after Rossi *et al.*, 1986; Liferovich *et al.*, 2006a and https://www.mindat.org/min-2414.html).

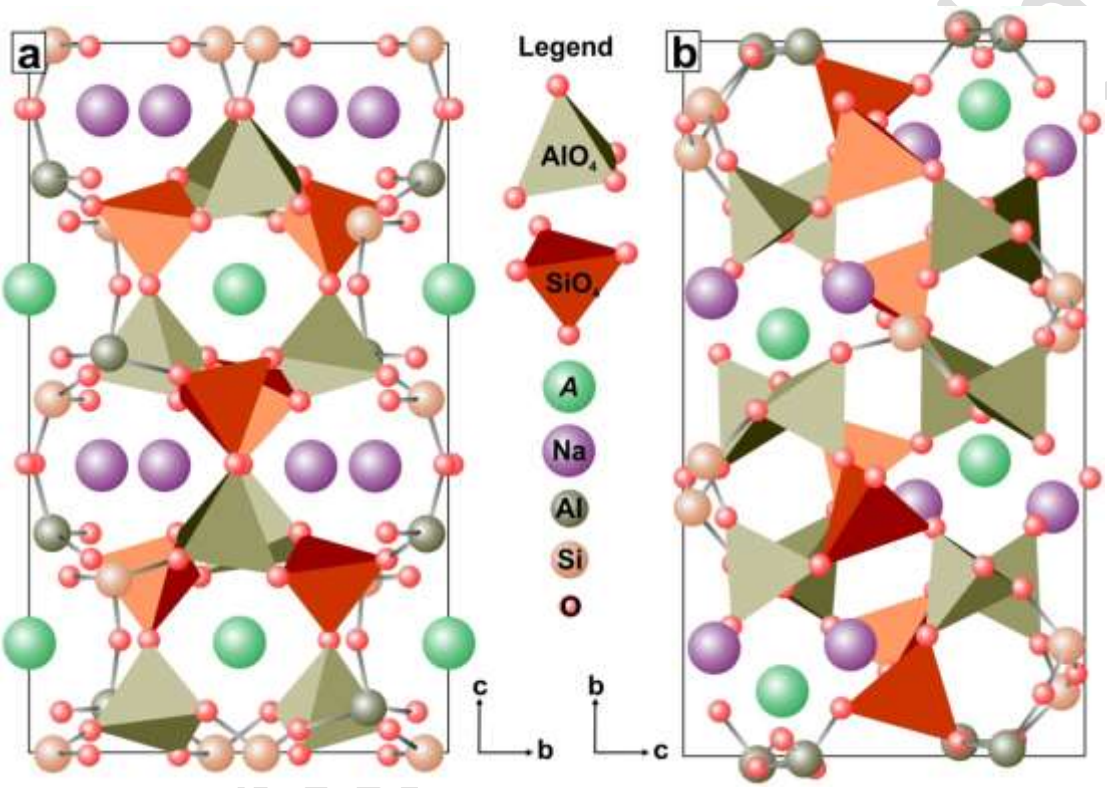

Fig. 2 Geological position of the Čerťák teschenite sill (modified according to Cháb *et al.*, 2007).

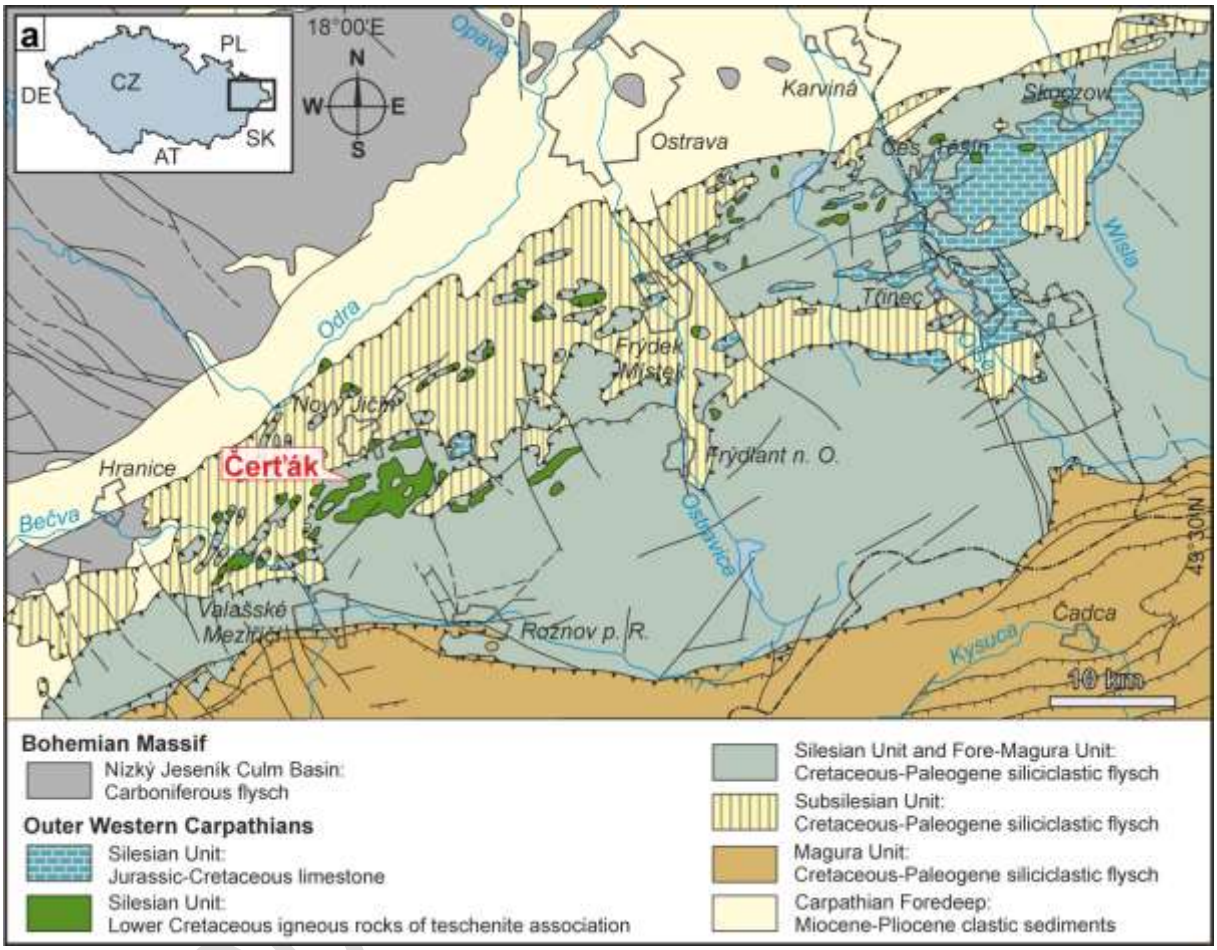

Fig. 3 (a, b) Macroscopic appearance of the studied teschenites (samples Č7 and Č10). Pseudomorphs with stronalsite (marked with red arrows) occur mostly in the marginal parts of leucocratic dykes or streaks. (c, d) Mineral association in the vicinity of a rectangular stronalsite-bearing pseudomorph in sample Č10: (c) plane-polarized light (PPL), (d) crossed polars (XPL). (e) The stronalsite-bearing rectangular pseudomorph at high magnification (PPL). (f) The inner part of a hexagonal skeletal pseudomorph in sample Č10. The Ba-rich stronalsite is turbid, whereas Ca-rich stronalsite is well transparent (PPL).

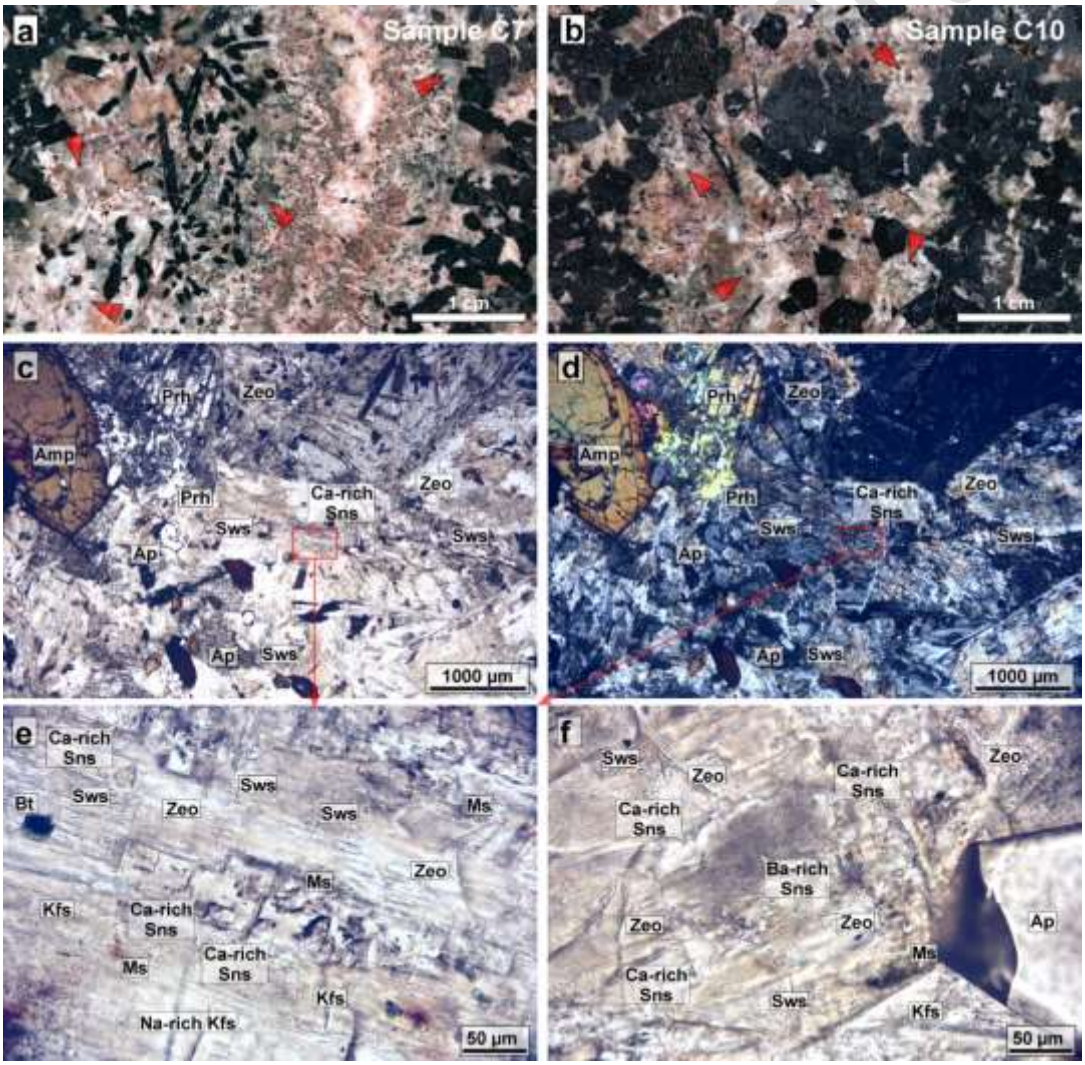

Fig. 4 BSE images of studied pseudomorphs from samples Č7 (a) and Č10 (b–d). (a) The Ba-rich stronalsite replaced along cracks and margins by natrolite, thomsonite-Ca, K-feldspar, celsian and muscovite. (b) A pseudomorph consisting of slawsonite (brighter in BSE) and Ba-rich stronalsite (slightly darker rim in BSE). Both Sr feldspars share subparallel cracks (or traces of cleavage inherited from mineral precursor) and are altered to a mixture of Na-Ca zeolites and muscovite. (c, d) Hexagonal skeletal pseudomorphs. The "atol" consists of slawsonite, Na-Ca zeolites and muscovite, the "inner lagoon" is filled by: (c) zeolites and Ca-rich stronalsite rimming porous brighter Ba-rich stronalsite, or by (d) hedenbergite, alkali feldspar and Na-Ca-zeolites.

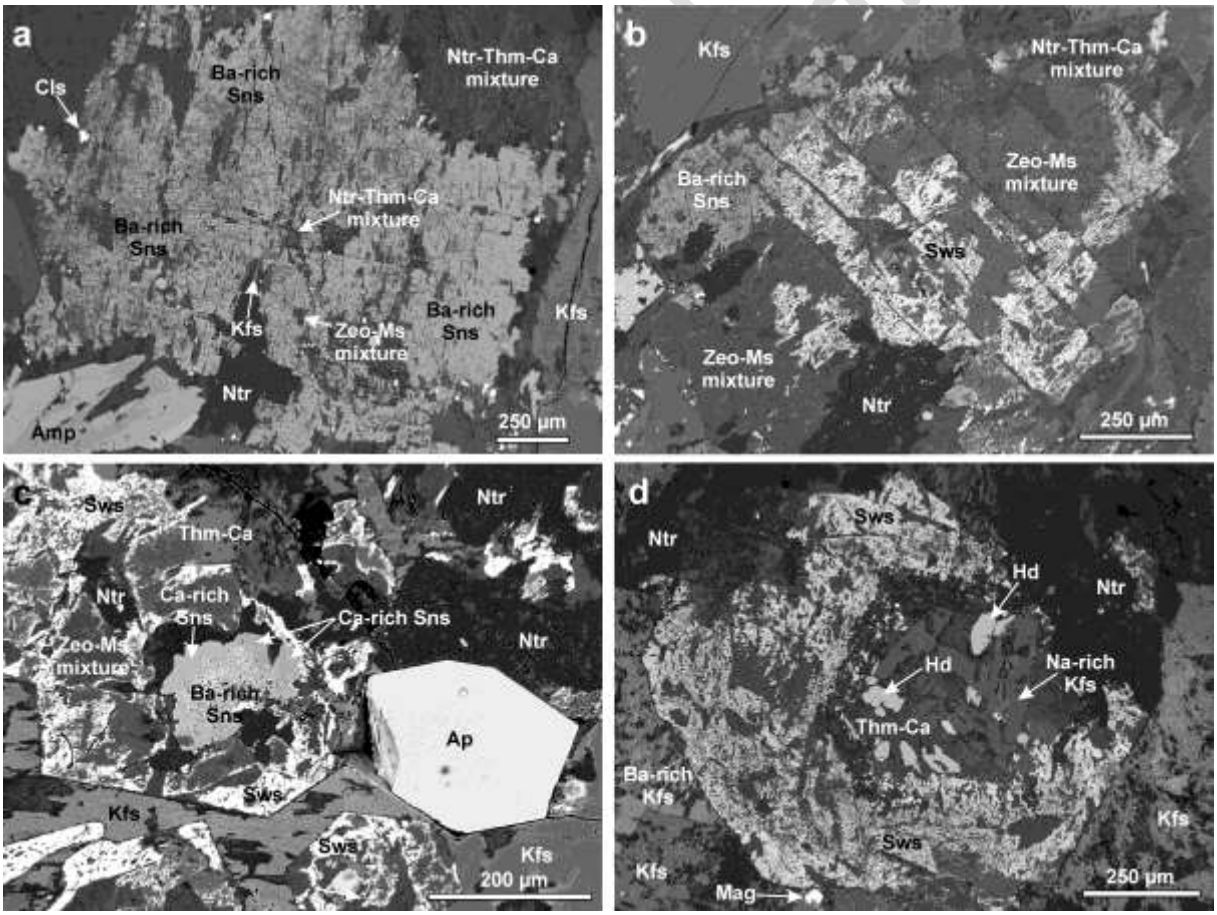

Fig. 5 Raman spectra of the studied Ba-rich stronalsite with ≤0.02 apfu Ca (a) and Ca-rich stronalsite with up to 0.23 apfu Ca (b) in sample Č10. The BSE images show the context of places, from which Raman spectra were collected.

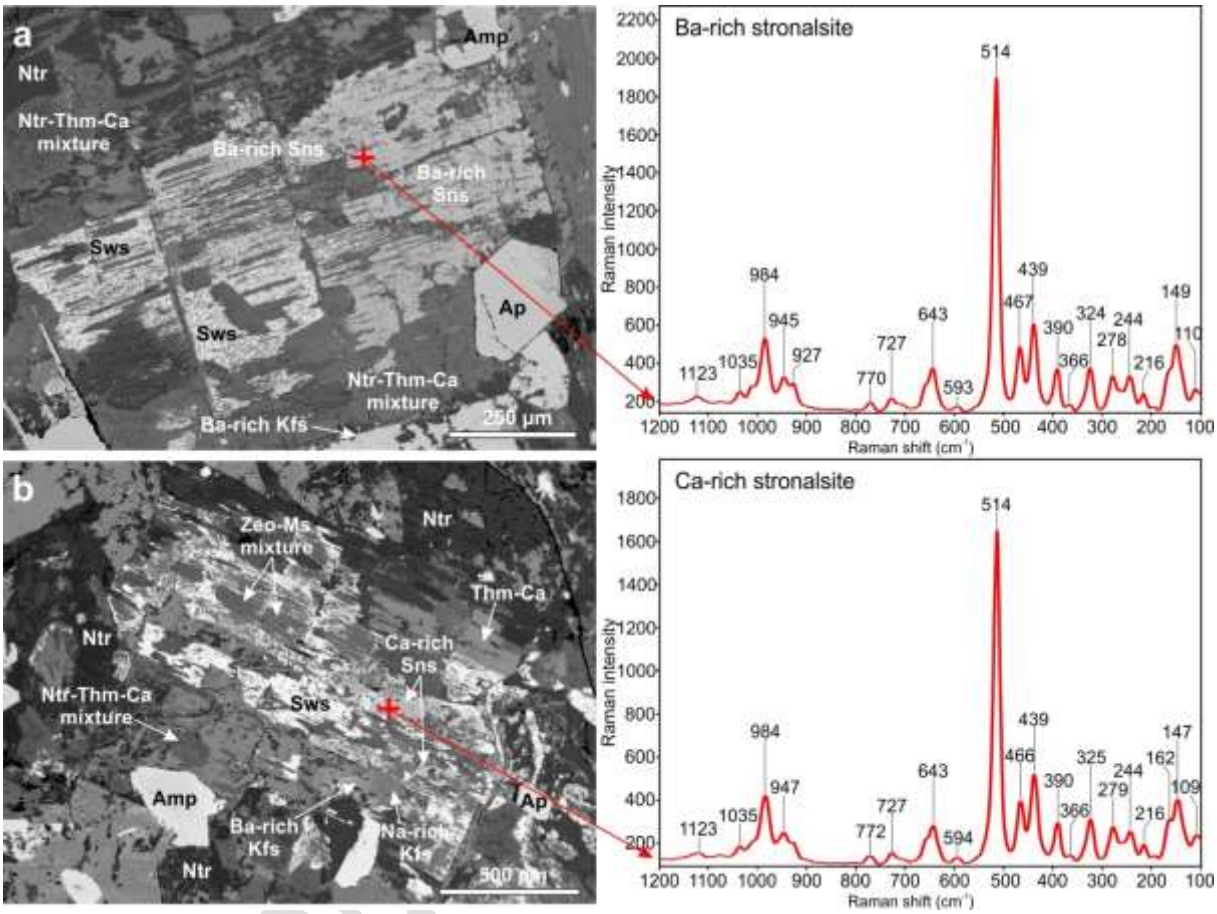

Fig. 6 Compositional variations of the studied stronalsite (a–c), slawsonite and celsian (d) and alkali feldspars (e). The dataset is supplemented with stronalsite compositions from the Rendai (Matsubara, 1985; Hori *et al.*, 1987), Punta del Peñón Blanco (Ahijado *et al.*, 2005), Khibina, Prairie Lake, Sakhorjok, Gremyakha-Vyrmes, Turiy Mys, Pilansberg (Liferovich *et al.*, 2006b) and Mikkelvik (Zozulya *et al.*, 2009) sites and slawsonite, celsian and Na-rich microcline analyses from the Čerťák site (Matýsek and Jirásek, 2016).

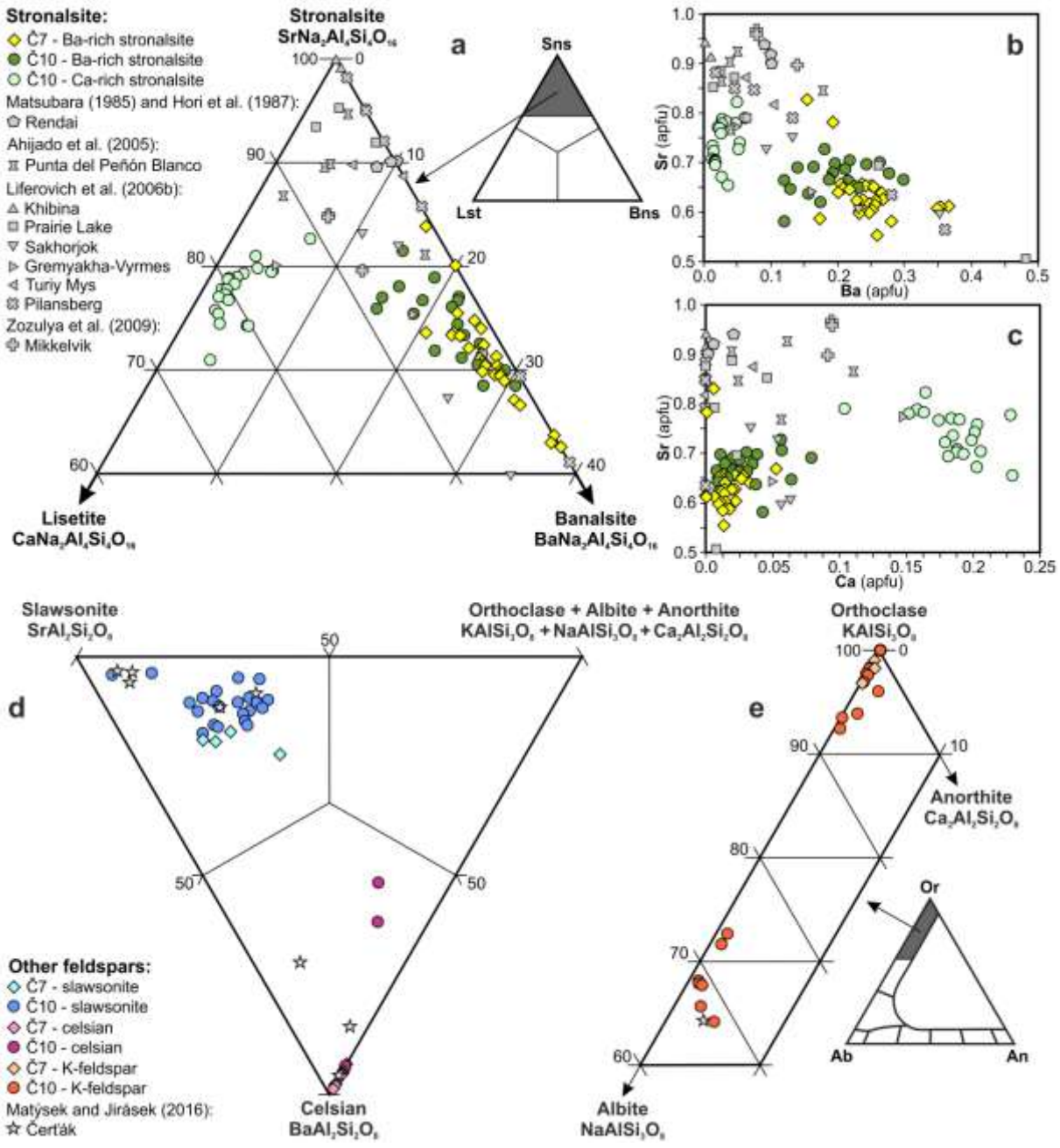

Fig. 7 Substitution diagrams showing the relationships among contents (apfu) of Ca and Sr, Ba, Na, Si, Al and Fe^{3+} in the studied stronalsite with calculated R^2 values: (a) diagram Ca vs. Sr + Ba, (b) Al + Ca vs. Si + Na, (c) Ca vs. Si, and (d) Ca vs. Al + Fe^{3+}. For key see Fig. 6a.

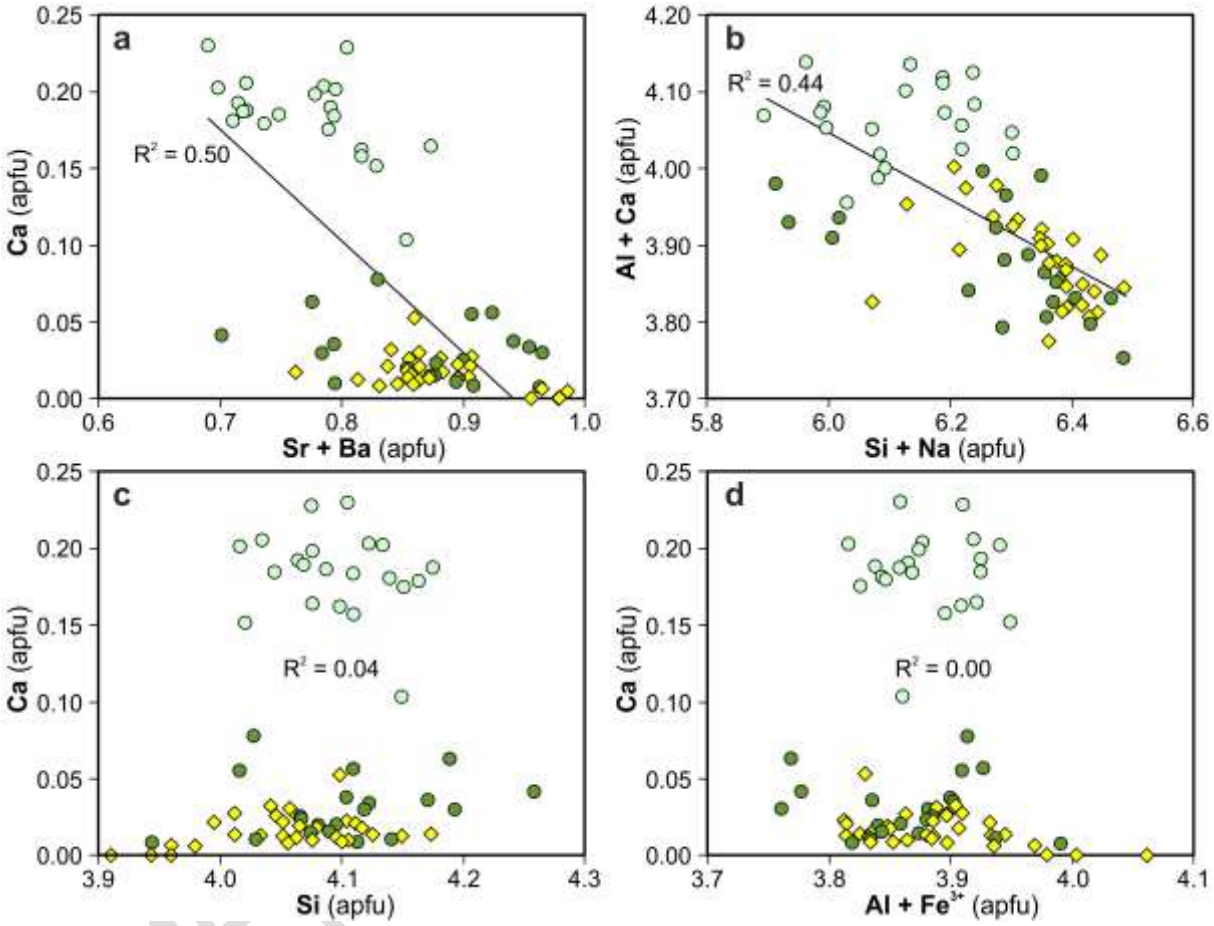

Table 1 Representative compositions of Ba- and Ca-rich stronalsite (apfu values are based on 16 oxygen atoms).

Mineral	**Ba-rich stronalsite**					**Ca-rich stronalsite**				
Sa./An.	**Č7/12**	**Č7/30**	**Č7/35**	**Č10/65**	**Č10/85**	**Č10/1**	**Č10/4**	**Č10/10**	**Č10/119**	**Č10/122**
SiO_2	40.44	37.30	38.43	40.19	42.96	41.38	40.30	41.12	41.43	40.79
Al_2O_3	31.11	32.00	32.69	33.13	32.11	32.60	33.18	32.75	31.98	32.12
Fe_2O_3	0.69	1.37	n.d.	n.d.	0.34	n.d.	n.d.	0.07	0.52	0.11
CaO	0.12	n.d.	0.05	0.73	0.40	1.69	1.72	2.15	1.74	0.95
SrO	9.32	10.08	13.91	11.87	10.10	11.94	12.61	11.28	12.10	13.39
BaO	6.44	8.92	3.84	3.57	3.10	0.44	0.35	0.93	0.35	1.57
Na_2O	11.13	10.92	11.35	11.95	10.55	10.73	11.02	11.04	9.76	9.54
K_2O	0.72	n.d.	0.04	0.08	0.94	0.41	0.28	0.25	0.47	0.22
Total	99.97	100.59	100.31	101.52	100.50	99.30	99.54	99.58	98.35	98.69
Si^{4+}	4.149	3.910	3.959	4.028	4.259	4.139	4.045	4.105	4.175	4.150
Al^{3+}	3.762	3.954	3.970	3.914	3.752	3.843	3.925	3.853	3.799	3.851
Fe^{3+}	0.053	0.108			0.026			0.005	0.040	0.009

∑*T* site	7.964	7.971	7.929	7.941	8.036	7.982	7.970	7.963	8.013	8.010
Ca^{2+}	0.013		0.006	0.078	0.042	0.181	0.185	0.230	0.188	0.104
Sr^{2+}	0.554	0.613	0.831	0.690	0.581	0.693	0.734	0.653	0.707	0.790
Ba^{2+}	0.259	0.366	0.155	0.140	0.120	0.017	0.014	0.036	0.014	0.063
∑*A* site	0.827	0.979	0.992	0.908	0.744	0.891	0.933	0.919	0.909	0.956
Na^{+}	2.213	2.219	2.267	2.321	2.027	2.080	2.144	2.136	1.907	1.881
K^{+}	0.094		0.005	0.010	0.119	0.052	0.036	0.032	0.060	0.029
Catsum	11.098	11.169	11.192	11.181	10.926	11.006	11.082	11.050	10.889	10.875
"Lst"	1.6	0.0	0.6	8.6	5.7	20.3	19.8	25.0	20.7	10.8
Sns	67.1	62.6	83.8	75.9	78.1	77.7	78.7	71.0	77.8	82.6
Bns	31.3	37.4	15.6	15.4	16.2	1.9	1.5	4.0	1.5	6.5

Abbreviations: n.d. = not detected.